Cribriform Pattern of The Prostate Adenocarcinoma: Sensitivity of Multiparametric MRI

Mustafa Bilal Tuna1*, Aydan Arslan[2], Yunus Baran Kök[3], Tunkut Doganca[4], Omer Burak Argun[5], Ilter Tufek[5], Betül Zehra Pirdal[6], Yesim Saglican[3], Can Obek[5], Ercan Karaarslan[7], Ali Riza Kural[5]

Background: The aim of this study was to investigate the diagnostic performance of mpMRI for detecting cribriform pattern prostate cancer.

Materials and Methods: This study retrospectively enrolled 33 patients who were reported cribriform pattern prostate cancer at final pathology. The localization, grade and volumetric properties of the dominant tumors and areas with cribriform pattern at the final pathological specimens were recorded and the diagnostic value of mpMRI was evaluated on the basis of the cribriform morphology detection rate. It was analyzed using Wilcoxon test, the Chi-square test and Fisher's Exact test. The significance level (*P*-value) was set at .05 in all statistical analyses.

Results: A total of 58 prostate cancer foci were (38 cribriform, 20 non-cribriform foci) identified on the final pathology. mpMRI identified 36 of the 38 cribriform morphology harboring tumor foci with a sensitivity of 94.7% (95% confidence interval 82.7–98.5%). In 17 of the 33 patients mpMRI detected single lesion and for these lesions; mpMRI identified cribriform morphology positive areas precisely in 15 patients with significantly low ADCmean and ADCmin values compared to the non-cribriform cancer areas within the primary index lesion ($P < .001$). For the remaining 16 patients with multiple lesions; all of the tumor foci that harboring cribriform morphology were identified by mpMRI but in none of them any ADCmean and ADCmin value divergence were detected between the cribriform and non-cribriform pattern tumor foci within the primary index lesion.

Conclusion: Cribiform pattern should be considered in single lesions with an area of lower ADC value on mpMRI.

Keywords: cribriform pattern, multiparametric MRI, prostate cancer

INTRODUCTION

MpMRI improves the detection of clinically significant prostate cancers and helps to prevent unnecessary biopsies.[1-3] PI-RADS v2.1 scoring system precisely predicts the clinically significant prostate cancer, with scores of 1 and 5 reflecting a very low and very high possibility of clinically significant cancer.[4] Four subtypes of Gleason pattern 4 are identified (cribriform, fused, glomeruloid and poorly formed) in recent years. The cribriform pattern is accepted more aggressive and more fatal than non-cribriform Gleason pattern 4 and is associated with increased risk of lymph node and distant metastasis, biochemical recurrence, and cancer-specific death.[5-7]
Recent studies have shown for active surveillance candidates; a cribriform pattern in the biopsy specimen is an exclusion criterion.[8] Therefore; identification of the cribriform pattern is crucial in terms of oncologic outcomes and clinical decision-making. However, data to date have claimed that cribriform pattern-predominant lesions are less visible on mpMRI and there are limited data on the radiologic evaluation of cribriform architecture.[9,10] In this study, we investigate the diagnostic effectiveness of mpMRI for detecting cribriform pattern prostate cancer.

MATERIALS AND METHODS

A total of 33 patients whose final pathologic specimen contains the cribriform pattern of prostate cancer after robot-assisted laparoscopic radical prostatectomy between September 2018 to February 2021 were included in this study. All patients had pre-operative biopsy-proven clinically significant prostate cancer. MpMRI was performed for all patients by the PI-RADS v2.1 guideline before the prostate biopsy and radical prostatectomy. All whole-mount step-section pathological slices were available and collected for pathological review. Patients who received neoadjuvant treatment

[1]Department of Urology, Acibadem Maslak Hospital, Istanbul, Turkey.
[2]Department of Radiology, Umraniye Training and Research Hospital; Istanbul,Turkey.
[3]Department of Pathology, Acibadem Mehmet Ali Aydinlar University School of Medicine, Istanbul, Turkey.
[4]Department of Urology, Acibadem Taksim Hospital, Istanbul, Turkey.
[5]Department of Urology, Acibadem Mehmet Ali Aydinlar University School of Medicine, Istanbul, Turkey.
[6]Department of Public Health, Cerrahpasa Faculty of Medicine, Istanbul University-Cerrahpasa, Kocamustafapasa, Fatih, 34098 Istanbul, Turkey.
[7]Department of Radiology, Acibadem Mehmet Ali Aydinlar University School of Medicine, Istanbul, Turkey.
*Correspondence: Department of Urology, Acibadem Maslak Hospital, Istanbul, 34457,Turkey.
Tel:+905052532047, Fax: +9002122190987, E-mail: mustafabilaltuna@gmail.com.
Received July 2022 & Accepted December 2022

Table 1. Imaging parameters of mpMRI

Sequences	Axial T2 TSE	Sagittal T2 TSE	Coronal T2	difussion	Axial T1 vibe	Axial T1 Dinamic	post-contrast axial T1vibe	post-contrast T1 fs coronal dixon
TR (msec)	3500,00	7320,00	7410	3700	5,70	4	5,72	530
TE(msec)	121,00	99,00	805	60	2,46	1,98	2,00	11
BW (hertz/pixels)	200,00	200,00	200	1414	590,00	500	590,00	303
interslice gap (%)	0,00	0,00	0	0	1,25	0,5	0,50	2,5
number of averages	2,00	1,00	1	1	1,00	1	1,00	1
time of acquisition (minutes)	2,70	1,25	1,34	3,00	1,14	3,4	1,14	2,2
FOV(mm)	200,00	220,00	200	200	320,00	200	320,00	340
NEX	2,00	1,00	1	1	1,00	1	1,00	1
NO of slices	24,00	24,00	24	24	88,00	24	88,00	20
Flip angle (FA)	160,00	160,00	160	160	10,00	12	10,00	140
voxel size(mm)	0.3x0.3x3	0.3x0.3x3	0.3x0.3x3	0.3x0.3x3	0.9x0.9x2,5	0.9x0.9x3	0.9x0.9x3	1x1x5
PAT mode	grappa	grappa	grappa	none	caipirinha	grappa	caipirinha	grappa
PAT factor	2,00	4,00	4	0	2,00	2	1,00	2
slice thickness(mm)	3,00	3,00	3	3	2,50	4	2,50	5
distance factor (%)	0,00	0,00	0	0	20,00	20	20,00	50
matrix	282x350	287x368	313x368	62x122	210x352	224x176	210x352	324x384

including androgen deprivation therapy or chemotherapy and underwent mpMRI after prostate biopsy were excluded from the study.

This study was approved by the Acibadem Mehmet Ali Aydınlar University Institutional Review Board (İstanbul, Turkey), (decision number:2022-05/10), and signed informed consent were collected from all subjects before MR imaging.

MRI Protocol and Image Analysis

MpMRI was performed with a 3.0-T MR scanner (Siemens Healthineers, Magnetom Skyra, Erlangen, Germany, or Siemens Healthineers) using either Gadovist (0.1mL / kg) or Dotarem, (0.2 mL/kg) as a contrast agent before the prostate biopsy. Detailed prostate mpMRI protocol is given in **Table 1**.

All images were evaluated by two experienced radiologists. The radiologists were blinded to the other radiologist's reports but after the evaluation of the dataset, consensus was achieved. The radiologists identified abnormalities that correspond to clinically significant prostate cancer. All tumor foci were recorded according to zone (central, peripheral, or transition zone), sector (anterior or posterior), regional part (apex, mid, or base), and laterality (left or right) using 41 sector maps in PI-RADS v2.1. To make sure that all readers were scoring the same area; each reader drew on the 41 sector map. The dimensions of the lesion(maximal axial,

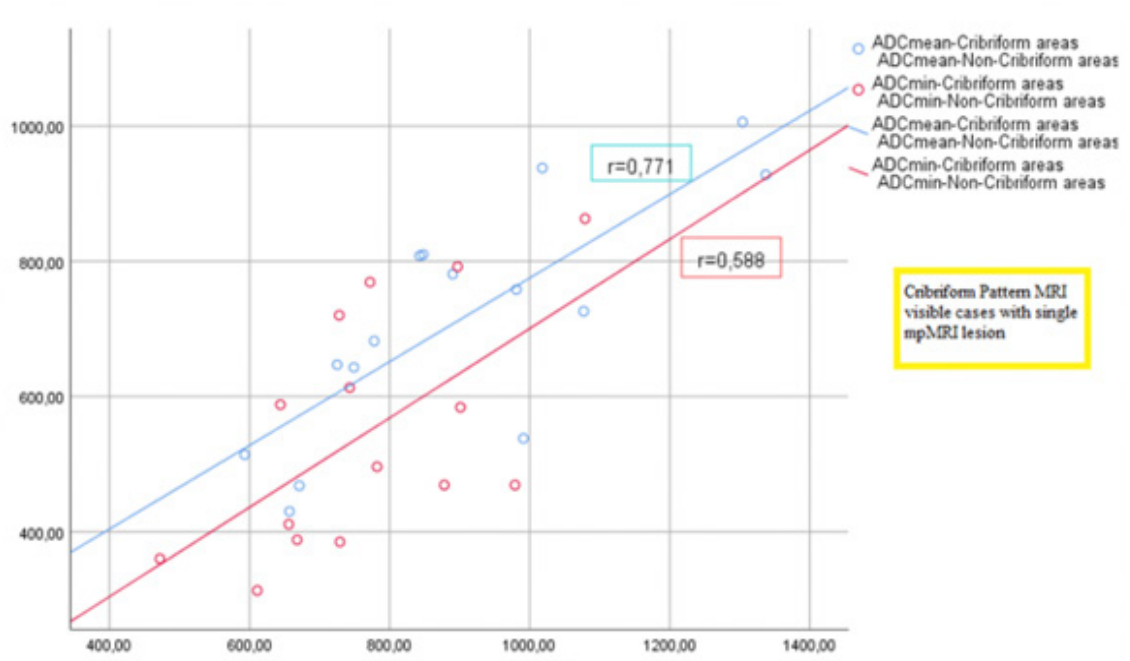

Figure 1. Correlations of ADCmean and ADCmin values between cribriform and non-cribriform areas within the primary index lesion in cases with single MRI lesion visible on mpMRI

Table 2. Clinical and pathologic characteristics of the study population

Age (years), Mean ± Std.deviation	63.6 ± 6.9
Time from MRI to Robot Assisted Radical Prostatectomy (days), Median (IQR)	51 (48-62.5)
PSA level (ng/mL), Median (IQR)	6.5 (4.9-10.3)
Final Pathologic Specimen (ISUP Grade), n (%)	
ISUP Grade 2	18 (54.5%)
ISUP Grade 3	11 (33.3%)
ISUP Grade 4	1 (3%)
ISUP Grade 5	3 (9.1%)
Prostate Volume (cm3), Median (IQR)	45 (36-53.5)
Tumor volume (cm3), Median (IQR)	4 (2.3-6.3)
Tumor ratio (tumor volume/prostate volume), Median (IQR)	9 % (3.6-15.8)
Cribriform morphology tumor burden (%), Median (IQR)	25% (12.5-50)
pT-stage, n (%)	
pT2	21 (63.6%)
pT3a	6 (18.1%)
pT3b	6 (18.1%)
pN-stage, n (%)	
n0	30 (90.9%)
n1	3 (9.1%)
Surgical Margin Positivity, n (%)	
Negative	28 (84.8%)
Positive	5 (15.1%)

perpendicular to axial plane, and coronal plane if possible) were calculated individually. All of the lesions PI-RADS ≥ 3 were scored by a radiologist according to the PI-RADS v2.1. The ADC values for suspicious lesions were measured by marking these areas as a region of interest(ROIs) on the ADC map. Mean and minimum ADC values were recorded without knowing the pathological results after the consensus of all lesions. Lastly, all of the ROIs were depicted manually based on tumor foci and cribriform pattern positive areas depending on the final pathology specimen with knowledge of the pathology findings.

The mpMRI index lesion was defined as the target with the highest PI-RADS score. In case of 2 or more lesions with the same PI-RADS score exists; the one regarded as clinically more suspicious by the radiologist was recorded as an index lesion. The pathology index lesion was defined as the lesion with the highest ISUP Grade score.

Whole-Mount Histopathology

Radical prostatectomy specimens were sliced at 3 mm intervals from the apex to the base. Two experienced genitourinary pathologists reexamined all whole-mount step-section pathological slices according to the 2014 ISUP modified prostate cancer criteria. The pathological workup was blinded to radiology findings. Both pathologists looked at all cases and the consensus was reached.

All tumor foci and cribriform pattern areas within each radical prostatectomy specimen were determined and mapped in different colors(blue&red) to a gross histopathology image that is routinely saved for each patient. From the total pathology specimen, the largest diameter of each lesion, histological type and grade, location of tumor foci, tumor spread, tumor volume, surgical margin status, lymph node involvement, and staging were documented. Cribriform pattern tumor burden ratio is defined as the percentage of cribriform pattern positive tumors in the total cancer amount(including ≥ Gleason 3) of the final pathology specimen.

2.4 Statistical Analysis

SPSS v.21 (SPSS Inc., Chicago, IL, USA) was used for statistical analysis. Shapiro-Wilk tests, histograms, and probability plots were used for assessing normality,. Results were presented as mean ± standard deviation for normally distributed variables, and median (IQR(Interquartile range)) for non-normally distributed variables. Categorical variables were presented with frequency and percentage. Comparisons of the groups for continuous variables were made by the Mann-Whitney U test. Differences between the two paired groups were tested using the Wilcoxon test. The Chi-square test or Fisher's Exact test was used to analyze categorical variables. Correlation coefficients were determined using Spearman rho. All tests are two-sided and the significance level was accepted as $P < .05$.

Table 3. MpMRI characteristics of the cribriform and non-cribriform tumor foci that were visible on mpMRI

Categories	All tumors foci visible on mpMRI (53)	Cribriform foci visible on mpMRI (36)	Non-Cribriform foci visible on mpMRI (17)	*P*
Diameter (MRI) (mm), Median (IQR)	12 (9-16)	13 (9.3-18.8)	10 (8.5-13)	.0541
Diameter (final pathology) (mm) Median (IQR)	13.3 (10.5-17.3)	14.5 (11.6-20.5)	10.8 (8.9-13.3)	.0021
mpMRI lesions, n (%)				
PI-RADS 3	6 (11.3%)	2 (5.3%)	4 (23.5%)	.0763
PI-RADS 4	31 (58.5%)	19 (52.8%)	12 (70.6%)	.2192
PI-RADS 5	16 (31.4%)	15 (44.1%)	1 (5.9%)	.0092
Localization, n (%)				
Basis	17 (32.1%)	12 (33.3%)	5 (29.4%)	.7212
Mid	24 (45.3%)	15 (41.7%)	9 (52.9%)	
Apex	12 (22.6%)	9 (25%)	3 (17.6%)	
Peripheral Zone	50 (94.3%)	36 (100%)	14 (82.4%)	.0293
Transitional Zone	3 (5.7%)	0 (0%)	3 (17.6%)	

1Mann Whitney *U* test, 2Chi square test, 3Fisher exact test

Table 4. Comparison of cribriform and non-cribriform areas in cribriform pattern visible cases on mpMRI with single mpMRI lesion and cases with multipl mpMRI lesion

Categories (n)	Cribriform areas Median (IQR)	Non-Cribriform areas Median (IQR)	*p*	Correlation r	*p*
All cases (n=31)					
ADCmean (μm²/s),	730 (643-848)	802 (700-991)	< .0011	0.834	< .0012
ADCmin (μm2/s),	611 (469-756)	721 (611-878)	< .0011	0.620	< .0012
Cribriform Pattern mpMRI visible cases with single mpMRI lesion (n=15)					
ADCmean (μm²/s)	726 (538-810)	848 (725-1018)	< .0011	0.771	.0012
ADCmin (μm²/s)	496 (388-720)	743 (656-897)	< .0011	0.588	.0212
Cases with Multiple mpMRI lesion (n=16)					
ADCmean (μm²/s)	755 (673-937.3)	755 (673-937,3)	1.001	1.00	-
ADCmin (μm²/s)	666 (519.3-756)	666 (519.3-756)	1.001	1.00	-

1Wilcoxon test, 2Spearman correlation

Results

In 33 patients a total of 58 PCa foci were(38 cribriform, 20 non-cribriform foci) identified on the final pathology specimen obtained after robot-assisted radical prostatectomy. The clinical and pathological characteristics of the whole study group are shown in **Table 2**. MpMRI index lesion was accordant with the prostatectomy index lesion in 31 of 33 cases (94%). MpMRI precisely identified 36 of the 38 cribriform morphology harboring tumors with a sensitivity of 94.7% (95% confidence interval 82.7–98.5%) in 31 of 33 patients (94%). On the other hand; mpMRI identified 17 of the 20 non-cribriform morphology tumors precisely. When the diameters of non-cribriform and cribriform tumor foci that were visible on mpMRI were examined, no difference was found with mpMRI, but the mean diameters of cribriform pattern harboring tumor foci were higher in the final pathology (respectively $P = .054$, $P = .002$).

In our whole study group; cribriform pattern harboring tumor foci is more frequently located in PI-RADS 5 lesions compared to non-cribriform tumor foci ($P = .009$). ISUP Grade of the cribriform pattern positive tumors visible on mpMRI was 2 in 18 foci, 3 in 13 foci, 4 in 2 foci, and 5 in 3 foci. ISUP Grade of the non-cribriform pattern positive tumors visible on mpMRI was 1 in 6 foci, 3 in 7 foci,3 in 3 foci, and 5 in 1 focus. All of the cribriform morphology positive and mpMRI visible tumor foci were located in the peripheral zone. Non-Cribriform morphology positive and mpMRI visible tumor foci were located in the transitional zone for 3 (17,6%) foci and peripheral zone for 14 (82,4%) foci. MpMRI characteristics of the cribriform and non-cribriform tumor foci that were visible on mpMRI are shown in **Table 3**.

In 2 of the 33 cases, mpMRI could not detect cribriform morphology positive areas. One of these patients' pre-operative mpMRI detected mid anterior located PI-RADS 4 lesion with a 9x8 mm diameter. In this case, final pathology revealed; pT2, ISUP Grade 2 prostate adenocarcinoma with a total of 1.6 cm3 tumor volume. Although preoperative mpMRI was concordant with the primary index lesion of the final pathology; mpMRI could not detect the apical anterior located small cribriform morphology positive area. For this case, the cribriform tumor burden ratio was 5%. The other patient's pre-operative mpMRI detected a mid-anterior located 10x7 mm PI-RADS 4 lesion and final pathology revealed pT2, ISUP Grade 2 prostate adenocarcinoma with a total of 6.1 cm3 tumor volume. For this patient, pre-operative mpMRI was accordant to the primary index lesion of the final pathologic specimen, but could not detect cribriform morphology positive small area that was located at the left apical region of the prostate. In this case, the cribriform tumor burden was 10%. On the other hand, 2 in the 33 cases mpMRI could not identify the primary index lesion of the final pathology specimen. In one of these cases, pre-operative mpMRI detected a mid posterior located PI-RADS 4 lesion with an 8x5 mm diameter. For this case; the final pathology revealed pT2, ISUP Grade 2 prostate adenocarcinoma with a total of 0.6 cm3 tumor volume. In this case, pre-operative mpMRI could not detect the primary index lesion that was located in the mid apical posterior aspect of the prostate but only identified the cribriform morphology positive area that was located at the mid posterior part of the prostate. In this case; the cribriform tumor burden was 10%. The other patient's pre-operative mpMRI detected a right mid-lateral located PI-RADS 4 lesion with a 6x4 mm diameter. In this case, the final pathology revealed pT2, ISUP Grade 4 prostate adenocarcinoma with a total of 1.5 cm3 tumor volume. For this case; the final pathology revealed multiple tumor foci that were located at the left mid, right mid posterior, right mid-lateral, and right apical region of the prostate and mpMRI detected only cribriform morphology positive area located at the right mid-lateral region of the prostate. The cribriform tumor burden ratio of this case was 45%. In 17 of the 33 cases, mpMRI detected a single lesion (6 PI-RADS 5, 11 PI-RADS 4) and among these cases, mpMRI identified cribriform morphology positive areas precisely in 15 patients. These cribriform positive area's ADCmean and ADCmin values were significantly low compared to the non-cribriform cancer areas within the primary index lesion. For the remaining 16 patients with multiple lesions (10 PI-RADS 5, 20 PI-RADS 4, 6 PI-RASD 3); all of the tumor foci that harbored cribriform morphology were identified by mpMRI but in none of them any ADCmean and ADCmin value divergence were detected between the cribriform pattern tumor foci within the primary index lesion and primary index tumor.

When the median ADCmean and ADCmin values in the cribriform and non-cribriform areas were examined in these 15 patients with single mpMRI lesion, it was found that the median ADCmean and ADCmin values in the cribriform areas were significantly low (retrospectively $P < .001$, $P < .001$) when compared to the non-cribriform tumor areas within the primary

index lesion. In these 15 patients with single mpMRI lesion; there was a high positive correlation (r = 0.771, $P < .001$) between ADCmean values in cribriform and non-cribriform areas, and a moderate positive correlation between ADCmin values (r = 0.588, $P = .012$) (**Table 4, Figure 1**). For the remaining 16 patients with multiple lesions (10 PI-RADS 5, 20 PI-RADS 4, 6 PI-RASD 3); all of the tumor foci that harbored cribriform morphology were identified by mpMRI but in none of them any ADCmean and ADCmin value divergence were detected between the cribriform pattern tumor foci and non-cribriform pattern tumor foci within the primary index lesion. On the other hand; the median cribriform pattern tumor burden ratio was 40% (IQR 25-50) in cases with mp MRI visible cases with single mpMRI lesion and 17.5% (IQR 10-57.5) in cases with multiple mpMRI lesions and no statistical difference was found between them ($P = .106$).

DISCUSSSION

In the PI-RADS v2.1 era; the pooled sensitivity and specificity of mpMRI for detecting prostate cancer are 89% and 73% respectively.[1-3] Despite these advantages; tumor volume, tumor density, Gleason score, and tumor heterogeneity with underlying clinical features (presence of cribriform and intraductal carcinoma) can affect the tumor visibility.[2,11-13]

Cribriform morphology can be defined as having moderately differentiated glands ranging from small to large, growing in spaced-out infiltrative patterns.[14] Moreover; the ISUP conference in 2014 arrived at a consensus that; cribriform glands should be assigned as Gleason pattern 4, regardless of morphology.[15] In addition to that; to improve the prostate cancer screening for initial prostate biopsy; the ERSPC Rotterdam risk calculator was updated in 2014 and stated that: the presence of cribriform or intraductal carcinoma should be defined as high-risk prostate cancer.[16]

The visibility of the Gleason 4 pattern varies depending on the morphologic features. Recently Aydan et. reported their experience in 58 men with 112 clinically significant prostate cancer foci to investigate the MpMRI visibility of prostate cancer according to the underlying histopathological variances. They concluded that; although statistically not significant, clinically significant prostate cancer with cribriform component and without any intraductal or cribriform component are more likely to harbor mpMRI invisible features than the intraductal pattern.[13] Moreover; it is noteworthy to mention recent reports on larger cohorts of patients highlighting the relatively high incidence of high-grade prostate cancer with cribriform morphology in patients with negative mpMRI. According to recent studies, cribriform pattern dominant prostate cancer is usually not visible at imaging and even on diffusion-weighted images of mpMRI. In this respect; quantitative analyses of mpMRI has shown encouraging results in peripheral tumor characterization.[17] The visibility of pure cribriform pattern tumors is reported % at 17 on MRI, which was significantly lower than other Gleason 4 pattern subtypes independent of tumor size.[10] The mechanism of the decreased visibility is unknown but theoretically attributed to the relatively larger luminal perforations and fewer epithelial cells of cribriform morphology.[9]

Gao J. et al. retrospectively collected the data of 215 prostate cancer patients who received mpMRI examination, systematic biopsy combined with targeted biopsy, radical prostatectomy, and final ISUP scores 2 and 3. In this study; cribriform morphology was detected in 110 of 215 patients (51.2%). They concluded that: prostate-specific antigen density ($P = .003$), Prostate Imaging Reporting and Data System score ($P < .001$) and maximal biopsy Gleason score ($P = .004$) were independent predictors for presence of cribriform morphology.[18] Prendeville et al. reported their prospective study that compares biopsy detection of intraductal and cribriform pattern prostate cancer in MpMRI positive and negative regions of the prostate in 151 patients. Intraductal/cribriform positive tumor was detected in 23 cases. For these cases; the prior 12-core systematic biopsy was negative in 8 and ISUP Grade 1 in 11 cases. They concluded that; the intraductal/cribriform pattern was significantly associated with PI-RADS score 5 and decreasing ADC values. This study shows the ability of MpMRI targeted biopsy to detect high-risk intraductal/cribriform Gleason pattern 4 prostate cancer.[19] Computer aided diagnostic (CAD) system assistance for fusion prostate biopsy has shown to be more effective in identification of clinically significant prostate cancers. CAD-assisted analyses provide enhanced graphic visualization and more precise spatial contouring of the lesion. These advantages of this system; instantly facilitate the detection of targeted areas; particularly in PI-RADS ≤ 3 lesions.[20] Moreover; Tonttila et al; reported their experience to assess the diagnostic ability for detecting cribriform patterns and intraductal carcinoma in 124 patients that underwent mpMRI before radical prostatectomy. They showed that mpMRI detected cribriform pattern and intraductal carcinoma with 90.5% sensitivity.[21] Our results correspond with their findings. In our study; we determined that; MpMRI precisely identified 36 of the 38 cribriform morphology harboring tumors (%94.7) in 31 of 33 patients (94%). There is a close inverse correlation between quantitative ADC measurement and clinical aggressiveness and Gleason Score. However, literature to date advocates that; there is no significant difference between the ADCmean between the cribriform-positive and non-cribriform prostate cancer. Tonttila et al. noticed a similar correlation between ADC values and clinical adverse events, but the range was so wide to show its clinical value. They stated that; the ADC value is not a marker to differentiate ISUP group 2 tumors with cribriform and intraductal carcinoma.[21] Similarly; Hurrel SL et al. did not find a correlation between the ADC values for Gleason pattern 4 with and without cribriform architecture and intraductal carcinoma.[22] Gao et al. retrospectively reported their data to investigate the diagnostic performance of Ga68 PSMA PET/CT in a total of 49 patients with 62 lesions. From these lesions, 37(59.7%) in 34 patients (69.4%) they detected cribriform morphology. Although they found that; ADCmean and ADC10% of were similar between cribriform positive and non-cribriform groups ($P > .05$); they showed that PSMA was significantly overexpressed in cribriform-positive prostate cancer ($P = .003$) and SUVmax was a significant predictor of cribriform morphology ($P < .001$).[23] Our results do not correspond with the previous studies on some points. In 17 of the 33 patients with a single mpMRI lesion; mpMRI detected a single lesion (6 PI-RADS 5, 11 PI-RADS 4), and for these lesions; mpMRI identified cribriform morphology posi-

tive areas precisely in 15 patients. For these 15 cases; the cribriform positive area's ADCmean and ADCmin values were significantly low compared to the non-cribriform cancer areas within the primary index lesion. On the other hand, in 16 patients with multiple lesions (10 PI-RADS 5, 20 PI-RADS 4, 6 PIRASD 3); all of the tumor foci that harbored cribriform morphology were identified but in none of them any ADCmean and ADCmin value divergence were detected between the cribriform pattern tumor foci within the primary index lesion and primary index tumor. This may be explained by the clustering of the cribriform pattern cells in a single lesion rather than dispersing around into multiple lesions. The strengths of our study are the detailed MRI analysis by two experienced radiologists and whole-mount histopathology of the primary tumor including cribriform architecture. Moreover, whole-Mount histopathology was evaluated based on identifying cribriform morphology by two experienced genitourinary pathologists to provide interobserver reliability. The main limitation of this study was the small (n = 33 men) sample size derived from a single tertiary center; therefore, adoption of our outcomes may not apply to community-based radiology and urology practice.

CONCLUSIONS

Despite reports of diminished visibility in the literature, multiparametric prostate MRI has high sensitivity and is an effective diagnostic technique for detecting cribriform pattern prostate cancer. In patients with a single lesion on pre-operative mpMRI, areas with lower ADCmean and ADCmin within the primary index lesion compared to the primary index lesion should be considered for cribriform pattern existence at the final pathology specimen. More randomized multi-center trials are needed to back up our findings.

CONFLICT OF INTEREST

None

FINANCIAL DISCLOSURE

None

REFERENCES

1. Weinreb JC, Barentsz JO, Choyke PL, et al. PI-RADS Prostate Imaging - Reporting and Data System: 2015, Version 2. Eur Urol. 2016 Jan;69(1):16-40. doi: 10.1016/j.eururo.2015.08.052. Epub 2015 Oct 1. PMID: 26427566; PMCID: PMC6467207.
2. Ahmed HU, El-Shater Bosaily A, et al.; PROMIS study group. Diagnostic accuracy of multi-parametric MRI and TRUS biopsy in prostate cancer (PROMIS): a paired validating confirmatory study. Lancet. 2017 Feb 25;389(10071):815-822. doi: 10.1016/S0140-6736(16)32401-1. Epub 2017 Jan 20. PMID: 28110982.
3. Kasivisvanathan V, Rannikko AS, Borghi M, et al.; PRECISION Study Group Collaborators. MRI-Targeted or Standard Biopsy for Prostate-Cancer Diagnosis. N Engl J Med. 2018 May 10;378(19):1767-1777. doi: 10.1056/NEJMoa1801993. Epub 2018 Mar 18. PMID: 29552975.
4. Turkbey B, Rosenkrantz AB, Haider MA, et al. Prostate Imaging Reporting and Data System Version 2.1: 2019 Update of Prostate Imaging Reporting and Data System Version 2. Eur Urol. 2019 Sep;76(3):340-351. doi: 10.1016/j.eururo.2019.02.033. Epub 2019 Mar 18. PMID: 30898406.
5. Iczkowski KA, Torkko KC, Kotnis GR, et al. Digital quantification of five high-grade prostate cancer patterns, including the cribriform pattern, and their association with adverse outcome. Am J Clin Pathol. 2011 Jul;136(1):98-107. doi: 10.1309/AJCPZ7WBU9YXSJPE. PMID: 21685037; PMCID: PMC4656017.
6. Dong F, Yang P, Wang C, et al. Architectural heterogeneity and cribriform pattern predict adverse clinical outcome for Gleason grade 4 prostatic adenocarcinoma. Am J Surg Pathol. 2013 Dec;37(12):1855-61. doi: 10.1097/PAS.0b013e3182a02169. PMID: 24145642.
7. Kweldam CF, Kümmerlin IP, Nieboer D, et al. Prostate cancer outcomes of men with biopsy Gleason score 6 and 7 without cribriform or intraductal carcinoma. Eur J Cancer. 2016 Oct;66:26-33. doi: 10.1016/j.ejca.2016.07.012. Epub 2016 Aug 11. PMID: 27522247.
8. Truong M, Frye T, Messing E, Miyamoto H. Historical and contemporary perspectives on cribriform morphology in prostate cancer. Nat Rev Urol. 2018 Aug;15(8):475-482. doi: 10.1038/s41585-018-0013-1. PMID: 29713007.
9. Truong M, Hollenberg G, Weinberg E, Messing EM, Miyamoto H, Frye TP. Impact of Gleason Subtype on Prostate Cancer Detection Using Multiparametric Magnetic Resonance Imaging: Correlation with Final Histopathology. J Urol. 2017 Aug;198(2):316-321. doi: 10.1016/j.juro.2017.01.077. Epub 2017 Feb 3. PMID: 28163032.
10. Truong M, Feng C, Hollenberg G, et al. A Comprehensive Analysis of Cribriform Morphology on Magnetic Resonance Imaging/Ultrasound Fusion Biopsy Correlated with Radical Prostatectomy Specimens. J Urol. 2018 Jan;199(1):106-113. doi: 10.1016/j.juro.2017.07.037. Epub 2017 Jul 18. Erratum in: J Urol. 2017 Dec 8;: PMID: 28728994.
11. Miyai K, Mikoshi A, Hamabe F, et al. Histological differences in cancer cells, stroma, and luminal spaces strongly correlate with in vivo MRI-detectability of prostate cancer. Mod Pathol. 2019 Oct;32(10):1536-1543. doi: 10.1038/s41379-019-0292-y. Epub 2019 Jun 7. PMID: 31175330.
12. Schieda N, Coffey N, Gulavita P, Al-Dandan O, Shabana W, Flood TA. Prostatic ductal adenocarcinoma: an aggressive tumour variant unrecognized on T2 weighted magnetic resonance imaging (MRI). Eur Radiol. 2014 Jun;24(6):1349-56. doi: 10.1007/s00330-014-3150-9. Epub 2014 Apr 1. PMID: 24687527.
13. Arslan A, Alis D, Tuna MB, Sağlıcan Y, Kural AR, Karaarslan E. The visibility

of prostate cancer concerning underlying histopathological variances: A single-center multiparametric magnetic resonance imaging study. Eur J Radiol. 2021 Aug;141:109791. doi: 10.1016/j.ejrad.2021.109791. Epub 2021 May 27. PMID: 34062471.

14. Gleason DF. Classification of prostatic carcinomas. Cancer Chemother Rep. 1966 Mar;50(3):125-8. PMID: 5948714.
15. Epstein JI, Egevad L, Amin MB, Delahunt B, Srigley JR, Humphrey PA; Grading Committee. The 2014 International Society of Urological Pathology (ISUP) Consensus Conference on Gleason Grading of Prostatic Carcinoma: Definition of Grading Patterns and Proposal for a New Grading System. Am J Surg Pathol. 2016 Feb;40(2):244-52. doi: 10.1097/PAS.0000000000000530. PMID: 26492179.
16. Roobol MJ, Verbeek JFM, van der Kwast T, Kümmerlin IP, Kweldam CF, van Leenders GJLH. Improving the Rotterdam European Randomized Study of Screening for Prostate Cancer Risk Calculator for Initial Prostate Biopsy by Incorporating the 2014 International Society of Urological Pathology Gleason Grading and Cribriform growth. Eur Urol. 2017 Jul;72(1):45-51. doi: 10.1016/j.eururo.2017.01.033. Epub 2017 Feb 2. PMID: 28162815.
17. Panebianco V, Barchetti G, Simone G, et al. Negative Multiparametric Magnetic Resonance Imaging for Prostate Cancer: What's Next? Eur Urol. 2018 Jul;74(1):48-54. doi: 10.1016/j.eururo.2018.03.007. Epub 2018 Mar 19. PMID: 29566957.
18. Gao J, Zhang Q, Fu Y, et al. Combined clinical characteristics and multiparametric MRI parameters for prediction of cribriform morphology in intermediate-risk prostate cancer patients. Urol Oncol. 2020 Apr;38(4):216-224. doi: 10.1016/j.urolonc.2019.09.002. Epub 2019 Oct 7. PMID: 31601518.
19. Prendeville S, Gertner M, Maganti M, et al. Role of Magnetic Resonance Imaging Targeted Biopsy in Detection of Prostate Cancer Harboring Adverse Pathological Features of Intraductal Carcinoma and Invasive Cribriform Carcinoma. J Urol. 2018 Jul;200(1):104-113. doi: 10.1016/j.juro.2018.01.081. Epub 2018 Feb 2. PMID: 29408568.
20. Ferriero M, Anceschi U, Bove AM, et al. Fusion US/MRI prostate biopsy using a computer aided diagnostic (CAD) system. Minerva Urol Nephrol. 2021 Oct;73(5):616-624. doi: 10.23736/S2724-6051.20.04008-4. Epub 2020 Nov 12. PMID: 33179868.
21. Tonttila PP, Ahtikoski A, Kuisma M, Pääkkö E, Hirvikoski P, Vaarala MH. Multiparametric MRI prior to radical prostatectomy identifies intraductal and cribriform growth patterns in prostate cancer. BJU Int. 2019 Dec;124(6):992-998. doi: 10.1111/bju.14812. Epub 2019 Jun 19. PMID: 31102571.
22. Hurrell SL, McGarry SD, Kaczmarowski A, et al. Optimized b-value selection for the discrimination of prostate cancer grades, including the cribriform pattern, using diffusion weighted imaging. J Med Imaging (Bellingham). 2018 Jan;5(1):011004. doi: 10.1117/1.JMI.5.1.011004. Epub 2017 Oct 27. PMID: 29098169; PMCID: PMC5658575.
23. Gao J, Zhang C, Zhang Q, et al. Diagnostic performance of 68Ga-PSMA PET/CT for identification of aggressive cribriform morphology in prostate cancer with whole-mount sections. Eur J Nucl Med Mol Imaging. 2019 Jul;46(7):1531-1541. doi: 10.1007/s00259-019-04320-9. Epub 2019 Apr 25. PMID: 31025048.